Journal of Materials Chemistry C

Accepted Manuscript

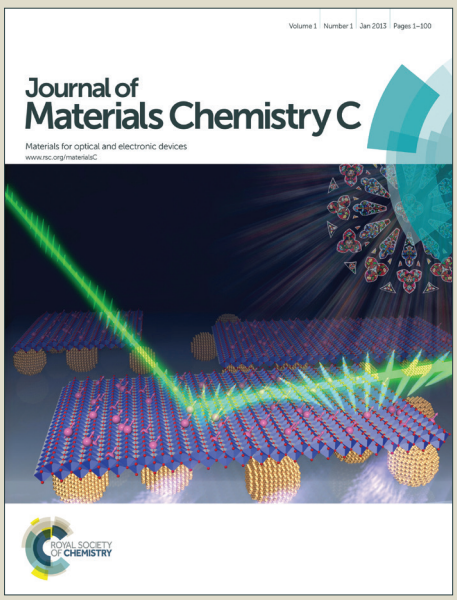

This is an *Accepted Manuscript*, which has been through the Royal Society of Chemistry peer review process and has been accepted for publication.

Accepted Manuscripts are published online shortly after acceptance, before technical editing, formatting and proof reading. Using this free service, authors can make their results available to the community, in citable form, before we publish the edited article. We will replace this *Accepted Manuscript* with the edited and formatted *Advance Article* as soon as it is available.

You can find more information about *Accepted Manuscripts* in the Information for Authors.

Please note that technical editing may introduce minor changes to the text and/or graphics, which may alter content. The journal's standard Terms & Conditions and the Ethical guidelines still apply. In no event shall the Royal Society of Chemistry be held responsible for any errors or omissions in this *Accepted Manuscript* or any consequences arising from the use of any information it contains.

ROYAL SOCIETY OF CHEMISTRY

www.rsc.org/materialsC

Journal Name

RSCPublishing

ARTICLE

Strong Enhancement of Second Harmonic Generation in the Nonlinear Optical Crystals: 2-Amino-3-nitropyridinium Halides (Cl, Br, I)

Tianliang Chen,[a] Zhihua Sun,[abc] Xitao Liu,[c] Jinyun Wang,[a] Yuelan Zhou,[d] Chengmin Ji,[a] Shuquan Zhang,[ab] Lina Li,[a] Junhua Luo,[*ab] and Zhong-Ning Chen[a]

Cite this: DOI: 10.1039/x0xx00000x

Received 00th January 2014,
Accepted 00th January 2014

DOI: 10.1039/x0xx00000x

www.rsc.org/

Three nonlinear optical (NLO) crystals of 2-amino-3-nitropyridinium halides (Cl, Br, I), which are assembled by anchoring the organic NLO chromophores into the halide anion frameworks through multicenter hydrogen bonds, have been successfully grown. Their optical transmittance window and cut-off wavelength have been investigated by the UV-visible-NIR studies. The Kurtz and Perry powder measurements disclose a large enhancement of their NLO activities, that is, second harmonic generation (SHG) efficiencies of 2-amino-3-nitropyridinium iodide are 1.5 times that of KDP, while, the corresponding values for the compounds of 2-amino-3-nitropyridinium chloride and 2-amino-3-nitropyridinium bromide are about 15 and 10 times, respectively. Further structure analyses and theoretical calculation reveal that such a distinct difference of the NLO behaviours results from their diverse coplanar alignments and dipole-dipole superposition, which is supposed to originate from the discrepant size of halide anions. It is believed that the enhancement of NLO response would point out a potential pathway to design new functional materials in the family of organic chromophores.

Introduction

Nonlinear optical (NLO) materials have attracted great attentions owing to their promising photonic applications in the field of optical information processing, optical switching, frequency conversion and terahertz (THz) wave generation, *etc*.[1-3] Generally, significant second-order NLO responses can be easily achieved in the compounds of chromophores. For compounds with large macroscopic NLO susceptibility ($\chi^{(2)}$) , one of the most essential characteristics for the chromophore is large molecular first-order hyperpolarizability, typically obtained in the planar delocalized π-electron systems. In inorganic materials, anionic groups with a π-conjugated system and a planar structure are only $[BO_3]^{3-}$, $[NO_3]^-$, and $[CO_3]^{2-}$, although some searchers have explored new materials with enhanced NLO activities by choosing the suitable size cation to induce the planar anionic group into the coplanar and parallel alignment.[4-6] Compared to inorganic NLO compounds, organic materials possess attractive advantages, including structure variety, high electronic susceptibility, and relative ease of device processing and so forth.[7-9] In order to obtain large macroscopic NLO efficiency, many methods have been used to enhance the molecular first-order hyperpolarizability, such as the increasing of the length for conjugated π-electron systems and the designing of dual charge-transfer chromophores (octupolar, star-shaped, Λ-shaped, X-shaped, Y-shaped, U-shaped, H-shaped and so on).[10-16] However, the achievement of large macroscopic susceptibilities remains a challenge, because of the possible non-optimal packing and even anti-parallel dipole arrangement of those chromophores in the crystals. Fortunately, these unfavourable arrangements can be considerably prevented by introducing inorganic anions, which can hinder mutual dipolar interactions between chromophores, and form supramolecular organic-inorganic hybrids.[17-19] Compared to pure organic or inorganic materials, one of the most interesting aspects for organic-inorganic hybrids is that their properties are strongly dependent on the included inorganic anion groups, which provide more opportunities for fine-tuning these NLO optical properties by the reasonable choice of anion groups to control the organic chromphore cations in optimal packing.[20-23] Although the rational assembly of the organic-inorganic NLO hybrids with dipolar NLO chromophores and suitable anions has been explored,[20-23] few researches are reported about the influences on the NLO

Journal of Materials Chemistry C Accepted Manuscript

efficiencies, caused by the different anions in the same main group.

2-Amino-5-nitropyridine, containing two electron-acceptors (NO_2 and NH^+) and one donor (amino group), has been artificially engineered into optimal arrangement to gain large macroscopic efficiencies in NLO materials by introducing zigzag chains or thick anionic walls.[24-32] As the isomer of the 2-amino-5-nitropyridine, 2-amino-3-nitropyridine (2A3NP) can easily be anchored into different anion host matrix by short and multiple hydrogen-bonds, while less NLO compounds based on it have been built compared to 2-amino-5-nitropyridium compounds.[33-35] Herein, we choose 2A3NP to construct NLO materials with the simple halide anions (Cl, Br and I). Single-crystal structures, thermal stabilities and optical properties were systematically investigated for these compounds. Further structure analyses and theoretical calculation reveal that their diverse coplanar alignments caused by the discrepant sizes of halide anions lead to such a distinct difference of the NLO responses. It points out a potential way to explore and design novel NLO material with enhanced NLO properties based on organic chromophores.

Experimental Section

All the chemical reagents were purchased as high purity (AR grade) and used without any further purification. 2-Amino-3-nitropyridinium chloride (2A3NPCl) was synthesized by dissolving 2A3NP in hydrochloric acid (HCl) solution with the molar ratio of 1:3 (0.01:0.03 mol) for 2A3NP and HCl at room temperature. The same preparation method was performed for 2-amino-3-nitropyridinium bromide (2A3NPBr) and iodide (2A3NPI) compounds. Crystals of 2A3NPCl, 2A3NPBr and 2A3NPI were grown up to 7× 8 × 3 mm^3, 10 × 10 × 2 mm^3 and 5 × 5 × 2 mm^3 (Figure S1, Supporting Information) by slow evaporation method, respectively.

Data collections for single crystal structures were corrected for Lorentz and polarization factors as well as for absorption by multi-scan method. All structures were solved by the direct methods and refined by full-matrix least-squares fitting on F^2 by SHELX TL software package.[36] All non-hydrogen atoms were refined anisotropically, and the positions of hydrogen atoms were generated geometrically. Crystallographic data and structural refinements for the two compounds are summarized in Table 1.

The purity of these crystals had been determinated by PXRD performed on a MiniFlex II X-ray diffraction instrument (Figure S2). Thermogravimetric (TG) and differential thermal analysis (DTA) measurements were carried out on a NETZSCH STA 449C with the heating rate of 10 ºC/min under nitrogen atmosphere (Figure S3). NLO properties were studied by Kurtz-Perry powder SHG test using an Nd: YAG laser (1064 nm) with input pulse of 450 mV. The micro-crystals of these three compounds and KDP standard sample with the same size of 250-310 μm were used to test their NLO efficiency. The three compounds with sizes in the range of 25-210 μm, sieved by a series of mesh, were utilized to perform the phase-matching experiment. The density functional theory (DFT) was used to optimize the corresponding crystal structures in order to calculate the first-order hyperpolarizability tensors by the hybrid functional B3LYP with the 6-311+ G (d) mode and the finite field method.

Table 1. Summary of crystallographic data for all three complexes

	2A3NPCl [34]	2A3NPBr	2A3NPI
Formula	$C_5H_6N_3O_2Cl$	$C_5H_6N_3O_2Br$	$C_5H_6N_3O_2I$
Formula w.t.	175.58	220.03	267.03
Crystal system	Monoclinic	Orthorhombic	Orthorhombic
Space group	$P2_1$	$Cmc2_1$	$P2_12_12_1$
a/Å	6.496(1)	6.(10)	6.702(3)
b/Å	9.040(4)	13.15(2)	9.243(4)
c/Å	7.263(1)	9.269(14)	13.476(5)
α/°	90	90	90
β/°	116.6(9)	90	90
γ/°	90	90	90
V/$Å^3$	381.3(3)	824(2)	834.8(6)
ρ_{calc}/gcm^{-3}	1.529	1.774	2.125
T(K)	293	293	173
Z	2	4	4
μ(mm^{-1})	2.417	4.946	3.793
F (000)	180	432	504
θ_{range} (°)	3-30	3.10-27.30	2.67-27.45
Gof on F^2	-	1.081	1.250
R_1(I>2σ(I))	0.026	0.0487	0.0240
wR_2 (all data)	-	0.1469	0.0997

Results and discussion

Crystal Structure Analysis.

Figure 1(a) shows the molecular arrangement of 2A3NPCl, which shows that each chlorine anion is connected with three 2A3NP cations by two strong hydrogen bonds N−H···Cl [N···Cl = 3.017 and 3.364 Å] and weak long hydrogen bonds C−H···Cl [C···Cl = 3.486 and 3.492 Å]. An alternating anion-cation chain is perfect parallelment along the polar axis (Figure S4), which is in favor of the charge transfer. Moreover, each chain is linked by the hydrogen bonds N2−H2···O2 [N2···O2 = 3.039 Å], which confirms the 2A3NP cation and chlorine anion to pack in the perfect two-dimensional layer structure. These perfect planes are parallel to the crystallographic plane defined by the ***b*** and (2***a*** + ***c***). Furthermore, the dihedral angle between the planes of the NO_2 group and the pyridine ring is 0.3º. However, there are no obvious hydrogen bonds established between adjacent layers.

Journal of Materials Chemistry C Accepted Manuscript

This journal is © The Royal Society of Chemistry 2012

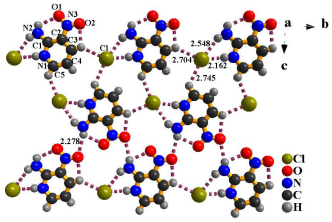

(a)

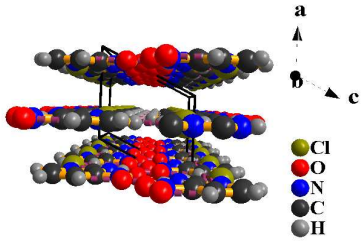

(b)

Figure 1. (a) Molecular arrangements on the (*b*, *c*) plane and (b) (*a*, *c*) plane in 2A3NPCl

Figure 2(a) shows the molecular arrangement of 2A3NPBr. Similar to that of 2A3NPCl, each bromide ion is connected with three 2A3NP cations with N−H···Br hydrogen-bonds and much weak interactioins of C−H···Br in which the 2A3NP cations are aligned in the same direction. An extremely similar anion-cation chain is formed along its *c*-axis, utilizing the strong hydrogen bonds of N2−H2A···O2 ($d_{N\cdots O}$ = 3.007Å) as the cohesion to form the perfect two-dimentional layer arrangement. Further, the dihedral angle between the plane of the NO_2 group and the pyridine ring is 0º. Different from that of 2A3NPCl, these perfect planes are parallel to the (*b*, *c*) plane, as shown in Figure 2(b). The distance between adjacent layers is 3.38 Å, indicating no hydrogen bonding interactions between the layers.

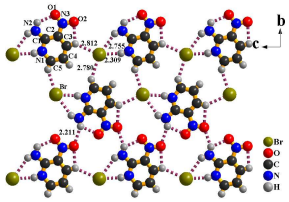

(a)

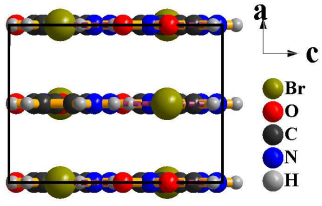

(b)

Figure 2. (a) Molecular arrangements on the (*b*, *c*) plane, (b) (*a*, *c*) plane in 2A3NPBr [N···Br = 3.179 and 3.518 Å], [C···Br = 3.591 and 3.617 Å]

Figure 3 shows the molecular arrangement of 2A3NPI crystal. As shown in figure 3(a), two pair cation-anions chains A and B are alternately stacked along *b*-axis interconnected through hydrogen bonds N2−H2B···I1. The 2A3NP cations of A and B chain are alternately stacked with a dihedral angle of 35.196° along the *c* axis. The 2A3NP cations are alternately stacked with a dihedral angle of 64.94° along *b*-axis. The above arrangement of the 2A3NP cations will lead to less favorable dipole-dipole superposition. The dihedral angle of the nitro group with respect to the planar heterocycle is 17.539°. Figure 3b shows the molecular arrangements on the *(b, c)* plane of A pairs. Each iodide ionic is linked with three 2A3NP cations by the hydrogen bonds N1−H1···I1 (N1···I1 = 3.462Å), N2−H2A···I (N2···I = 3.635 Å), C3−H4···I1 (C3···I1 = 3.879Å) and C5−H5···I1 (C5···I1 = 3.808 Å) to form two dimensional corrugated layer structure. Furthermore, the 2A3NP cations and iodide anions are not aligned as shown in figure 3b, which will be not in favour of the charge transfer. Therefore, unlike 2A3NP cations described in 2A3NPCl and 2A3NPBr, the 2A3NP cations in 2A3NPI are not coplanar aligned.

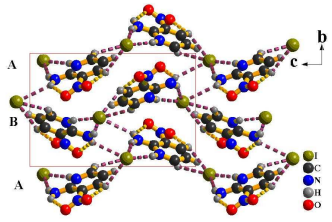

(a)

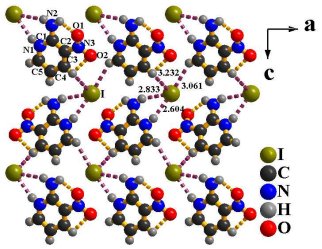

(b)

Figure 3 (a) Molecular arrangements on the (*b*, *c*) plane, (b) (*a*, *c*) plane in 2A3NPI.

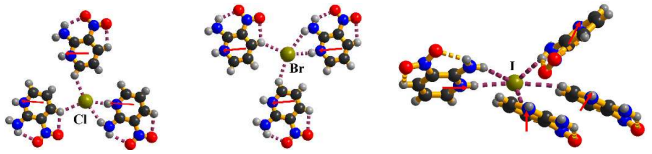

(a) (b) (c)

Figure 4. Alignment of the 2A3NP cations in three compounds. Similar frameworks are observed in both 2A3NPCl and 2A3NPBr, while 2A3NPI shows a quite different structure.

Very interestingly, our above structural investigations show that there are distinctive different arrangements for these three compounds: (1) all 2A3NP cations are coparallel in (*b*, *c*) plane

Journal of Materials Chemistry C Accepted Manuscript

and arranged in aligned fashion bonded through strong hydrogen bond N1−H1···X (Cl, Br) along the polar axis resulting in directional arrangement of the dipole moment for 2A3NPCl and 2A3NPBr; (2) all 2A3NP cations are arranged in different orientations and thus noncoplanar arrangement which leads to non-favourable dipole moment arrangements in 2A3NPI as in figure 3(a). Once the structures are examined more closely, one can find that the halogen ion play important roles in determining arrangements in the three compounds.

We suppose that such an above phenomenon might originate from the different ionic radii of the halide anions. On the one hand, possessing smaller ionic radii resulting in smaller van der Waals radius for Cl and Br, each halide anion (Cl^-, Br^-) was only connected with three 2A3NP cations through two strong hydrogen bonding N−H···X (Cl^-, Br^-) and two weak interactions C−H···X (Cl^-, Br^-) which are both paralleled to (b, c) plane (Figure 4(a) and 4(b)), leading to the coplanar and orientational arrangement of their dipole moments. However, due to the larger van der Waals radius of I in 2A3NPI, the more complicated interaction environment, where each iodide was linked with four 2A3NP cations by three strong hydrogen bondings N−H···I and two weak interactions C−H···I (Figure 4(c)), results in noncoplanar and non-favourable arrangement of dipole moment. On the other hand, 2A3NPI has the similar structure parameters as 2A3NPBr but differs only in the identity of the counter-ion. The volume of the unit cell is unexpectedly less by 10 Å for the iodide case, even though I^- ion has a larger ionic radius (2.20 Å) than bromide (1.96 Å). If 2A3NPI has the same packing arrangement as 2A3NPBr, there would lead to the over-jostling of 2A3NP cations, resulting in unstable status of the whole system for 2A3NPI. Subsequently, the 2A3NP cations will be rearranged to obtain more stable structure in 2A3NPI and there will be markedly distinction in molecular packing of 2A3NPI compared to 2A3NPBr. Furthermore, in order to further confirm the above hypothesis, the bond length and angles of hydrogen bonds (strong hydrogen bond N1−H1···I) of the assumed molecular arrangement in 2A3NPI which is the same as the 2A3NPBr, were calculated by functional B3LYP with the 6-311+ G (d) mode. As we can see in Table S1, if the molecular arrangement of 2A3NPI is similar with that of 2A3NPBr, the $d_{I\text{-}N2}$ in the assumed molecular arrangement of 2A3NPI is 3.91 Å, which is longer than the $d_{I\text{-}N2}$ 3.63 Å in 2A3NPI, indicating that there are weaker cation-anion interaction which would lead to an unstable system in 2A3NPI. Hence, such a non-favourable molecular arrangement in 2A3NPI may reduce the energy of the whole system and thus keep it into more stable status. It is supposed that these different arrangements would originate from the different size of the halogen ions, which not only optimize their crystal packing, such as a coplanar aligned in both 2A3NPCl and 2A3NPBr, but also exert great effects on their bulk second-order NLO properties, which needs further investigations.

Optical Properties Studies

Transmission spectra for three crystals performed in the wavelength range from 450 to 1500 nm are presented in Figure 5, which shows that the UV-Vis transparency cutoff wavelengths of as-grown 2A3NPCl, 2A3NPBr and 2A3NPI crystals occur at 432, 436 and 490 nm, respectively. The absence of absorption in the region below 1400 nm makes all of them possible to be used as NLO materials. [37] SHG properties of 2A3NPCl, 2A3NPBr and 2A3NPI crystals were also studied following the Kurtz and Perry powder technique.[38] Relative powder SHG intensities of 2A3NPCl, 2A3NPBr, and 2A3NPI are about 15, 10 and 1.5 times that of KDP as shown in Figure 6(a). Furthermore, the SHG intensities for 2A3NPCl, 2A3NPBr and 2A3NPI powders as a function of particle size indicate that their SHG intensities increase with particle sizes and approach almost saturated with particle size up to 200 μm, confirming their phase-matchable properties of Type I (see Figure 6b). Here, we discuss that the large differences of their NLO properties would be ascribled to the intrinsic difference of their crystal structures. In both 2A3NPCl and 2A3NPBr, their coplanar alignments of the 2A3NP cation along the same direction will be favorable to dipole-dipole superposition and lead to a complete additivity of the molecular β tensor components for the macroscopic $\chi^{(2)}$ susceptibility; while for 2A3NPI, it can be seen that 2A3NP cations are arranged not only without coplanarity, but also with less favorable dipole-dipole superposition, which remarkably hinder the charge-transfer interaction, weakening its macroscopic optical nonlinearities

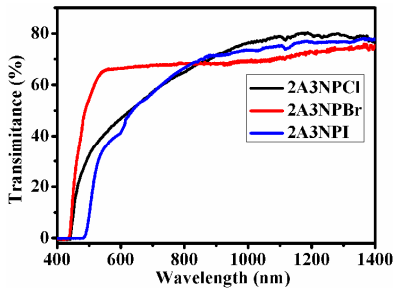

Figure 5. Transmission spectra performed on the crystal samples of 2A3NPCl, 2A3NPBr and 2A3NPI.

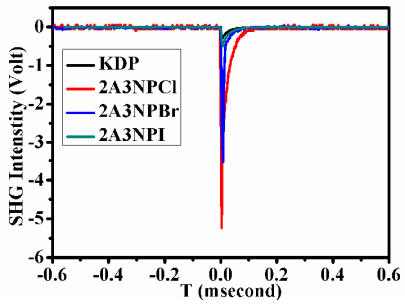

(a)

Journal of Materials Chemistry C Accepted Manuscript

This journal is © The Royal Society of Chemistry 2012

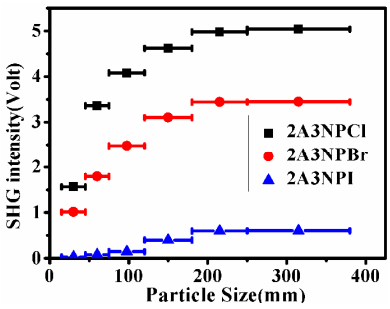

(b)

Figure 6(a) Oscilloscope traces of the SHG signals of KDP, 2A3NPCl, 2A3NPBr and 2A3NPI at the same particle size of 150–210 μm; (b) Phase-matching curves, i.e., particle size versus SHG response, for 2A3NPCl, 2A3NPBr and 2A3NPI.

Theoretical Calculation of First Hyperpolarizability

In order to probe the microscope nonlinearity of 2-amino-3-nitropyridinium halide salts, we calculated the first hyperpolarizability tensors of the geometry optimizations of these molecular structures by density functional theory (DFT), using the hybrid functional B3LYP with the 6-311+G (d) mode. During the determination of (*x*, *y*, *z*) directions in the Cartesian coordinate system, *z*-axis is pointed along the molecular polar axis and *y*-axis is fixed at the vertical direction. Therefore, 2A3NPX (X =Cl, Br and I) lies in *yz* plane, which may result in the largest components β_{ijk} in this plane. The results of the first-order hyperpolarizability β_{ijk}, and the angle (θ_p) between the vector part of the maximum first hyperpolarizability β_{max} and the dipole moment (μ) are listed in Table 3. For 2A3NPCl, the component β_{zzz} dominates the β_{tot} ($\beta_{tot} = (\sum \beta_i^2)^{1/2}$, $\beta_i = \beta_{iii} + \sum(\beta_{ijj} + \beta_{jij} + \beta_{jji})/3$) component reaching to 71.8%; for 2A3NPBr, the component β_{yyy} dominates the β_{tot} component reaching to 86%. In the other direction, the particular components are almost equal to zero for 2A3NPCl and 2A3NPBr. The above distribution of the components β_{ijk} can be attributed to unidirectional charge-transfer by the hydrogen bond between the 2A3NP cation and the halide anion (Cl^- and Br^-); while for 2A3NPI, these components are scattered in all directions. It can be also seen that the value of the maximum first hyperpolarizability β_{max} is 2A3NPBr ＞2A3NPCl ＞ 2A3NPI, while, the experimental value of their NLO efficiency is 2A3NPCl ＞2A3NPBr ＞ 2A3NPI. There is a contradiction between experimental macroscopic NLO efficiency and theoretical maximum first hyperpolarizability β_{max} for 2A3NPCl and 2A3NPBr. The reason for the higher SHG efficiency of 2A3NPCl crystals compared to 2A3NPBr crystals can be related to polar alignment of the chromophores in the crystalline lattice. In order to clearly determine polar alignment of the chromophores in the crystalline state, we calculated the angle between the direction of the maximum first hyperpolarizability β_{max} and the dipole moment μ. The direction of the maximum first hyperpolarizability β_{max} of 2A3NPCl molecule is aligned at a small angle of θ_p = 23.4° with the polar *b*-axis, which is considerably smaller than that for 2A3NPBr molecule with a large θ_p = 75.2 with the polar *c*-axis. Therefore, 2A3NPCl crystal has a highly polar alignment with a high order parameter $\cos^3(\theta_p)$ = 0.773, which is larger than that of 2A3NPBr crystal with a low order parameter $\cos^3(\theta_p)$ = 0.017.[39] Herein, even though the molecular nonlinearity is only half of that for 2A3NPBr crystals, 2A3NPCl can also exhibit a larger macroscopic NLO efficiency. For 2A3NPI, the non-coplanar arrangement and small molecular nonlinearity lead to the remarkable weakening of the NLO efficiency.

Table 3. Calculated the first-order hyperpolarizability β ($\times 10^{-30}$esu) and crystal second-order susceptibilities $\chi^{(2)}$ from molecules.

	2A3NPCl	2A3NPBr	2A3NPI
β_{xxx}	0	0	-0.53
β_{xxy}	-0.23	-0.05	1.87
β_{xyy}	0.01	0.01	-1.20
β_{yyy}	2.58	32.23	0.42
β_{zxx}	-0.22	-0.27	3.02
β_{xyz}	-0.01	0	-1.12
β_{zyy}	-3.96	6.95	0.59
β_{xzz}	0	0	-0.94
β_{yzz}	2.71	4.24	-0.35
β_{zzz}	-12.54	2.24	-1.34
β_{max}	14.30	34.94	1.41
β_{tot}	17.47	37.49	4.01
θ_p	23.4°	75.2 °	7.0 °
N	1.58	0.73	0.72
L	1.42	1.19	1.25
$\|\chi^{(2)}\|$	34.36	30.66	6.78
$\chi^{(2)}$(ex)	48 (3)	32(2)	4.8 (1)

Unit: N for 1021 cm3, $\chi^{(2)}$ for 10^{-9} esu.

Now we make comparisons between the theoretical and experimental NLO susceptibility. The NLO susceptibility of the bulk material can be estimated by following equation: [40-41]

$$\left\|\chi^{(2)}_{abc}(-2\omega,\omega,\omega)\right\| = NL\left\|\beta_{abc}(-2\omega,\omega,\omega)\right\|$$

Here, N can be calculated with N = $1/V_{cell}$ (V_{cell} is the volume of the unit cell of the crystal). L is the local field correction factor calculated from $L = f_a^{2\omega} f_b^{\omega} f_c^{\omega}$, and the $f_a^{2\omega} = (n_\omega^2 + 2)/3 = 3/(3-4\pi N\alpha_\omega)$, with the assumption of the Lorent-z-Lorenz local field, in which n_ω is the refractive index and α_ω is the first-order microscopic polarizability.[42-43] Here we make an approximation of $\alpha_{2\omega} = \alpha_\omega$ in calculation of L factor. The calculated value of $\| \chi^{(2)} \|$ is listed in Table 3 at an input wavelength of 1064 nm. The experimental value of $\chi^{(2)}$(exp) can be calculated with $\chi^{(2)}$ (exp) = b × $\chi^{(2)}$ (KDP) ($\chi^{(2)}$(KDP)= $2d_{36}$), where b is their NLO efficiency times that of KDP. The selected value d_{36} of KDP is the average value 1.6×10^{-9} esu, and thus, the experimental value $\chi^{(2)}$ (ex) are $48(3)\times10^{-9}$,

Journal of Materials Chemistry C Accepted Manuscript

$32(2)\times10^{-9}$ and $4.8(1)\times10^{-9}$ esu, for 2A3NPCl, 2A3NPBr and 2A3NPI, respectively. The calculated values almost agree with the experimental values.

Conclusions

In the present work, we have grown three NLO crystals built by the simple halogen anion with the 2-amino-3-nitropyridine nonlinear chromosphores to assemble different framework acentric structures by multicenter hydrogen bonds. The SHG measurements indicate that the 2A3NPCl, 2A3NPBr and 2A3NPI are all phase-matchable materials with the NLO activities of about 15, 10 and 1.5 times that of KDP. The difference of their NLO efficiency was caused by the diverse coplanar alignments and dipole-dipole superposition directed by the discrepant size of the halide anions. We therefore proposed that the moderate size of halogen anions could promote coplanar arrangement of the 2A3NP cation and dipole-dipole superposition to induce the enhancement of the macroscopic second-order optical nonlinearity, which would provide a clue for exploring new NLO materials with enhanced second harmonic generations.

Acknowledgements

This work was financially supported by the National Nature Science Foundation of China (21222102, 21373220, 51102231, 21171166 and 21301171), the 973 key programs of the MOST (2010CB933501 and 2011CB935904), the One Hundred Talent Program of the Chinese Academy of Sciences and the key project of Fujian Province (2012H0045). Dr. Sun thanks the support from "Chunmiao Project" of Haixi Institute of Chinese Academy of Sciences (CMZX-2013-002).

Notes and references

[a] Key Laboratory of Optoelectronic Materials Chemistry and Physics, Fujian Institute of Research on the Structure of Matter, Chinese Academy of Sciences, Fuzhou, Fujian， 350002, P.R. China. E-mail: jhluo@fjirsm.ac.cn. Fax: (+86) 0591-83730955. Tel: (+86) 0591-83730955.

[b] State Key Laboratory of Structural Chemistry, Fujian Institute of Research on the Structure of Matter, Chinese Academy of Sciences, Fuzhou, Fujian，350002, P.R. China.

[c] State Key laboratory of Crystal Material, Shandong University, Jinan, 250100, China.

[d] College of Chemistry and Chemical Engineering, Jiangxi Normal University, Nanchang, Jiangxi 330022, P. R. China.

† Electronic supplementary information (ESI) available: Photographs of crystal, PXRD pattern, CIF file, TG curves, CCDC 975900, 975902.

1 L. R. Dalton, P. A. Sullivan, D. H. Bale, *Chemical Rev*., 2010, **110**, 25.
1 Special Issue on Molecular Photonic Molecules, Materials, Devices: C.R. Acad, *Sci. Phys*., 2002, **3**, 403.
2 M. Lee, H. E. Katz, C. Erben, D. M. Gill, P. Gopalan, J. D. Heber, D. J. McGee, *Science*, 2002, **298**, 1401.
3 M. Jazbinsek, O. P. Kwon, C. Bosshard, P. Günter, *Handbook of Organic Electronics and Photonics*; Nalwa, S. H., Ed.; American Scientific Publishers: Stevenson Ranch, CA, 2008.
4 G. Zou, N. Ye, L. Huang, and X. Lin, *J. Am. Chem. Soc*., 2011, **133**, 20001.
5 S -J. Oh, D. W. Lee, and K. M. Ok, *Inorg. Chem*., 2012, **51**, 5393.
6 M.-H. Choi, S.-H. Kim, H. Y. Chang, P. S. Halasyamani, K. M. Ok, *Inorg. Chem*., 2009, **48**, 8376.
7 L. R.Dalton, P. A. Sullivan, B. C. Olbricht, D. H. Bale, J.Takayesu, S. Hammond, H. Rommel, B. H. Robinson, *Tutorials in Complex Photonic Media*; SPIE: Bellingham, WA, 2007.
8 E. Ishow, C. Bellaïche, L. Bouteiller, K. Nakatani, J. A. Delaire, *J. Am. Chem. Soc*., 2003, **125**, 15744.
9 V. G. Dmitriev, G. G. Gurzadyan, D. N. Nicogosyan, *Handbook of Nonlinear Optical Crystals* ; Springer-Verlag: New York, 1999.
10 K. M. Ok, P. S. Halasyamani, D. Casanova, M. Llunell, P. Alemany, S. Alvarez, *Chem. Mater*., 2006, **18**, 3176.
11 M. D. Donakowski, R. Gautier, J. Yeon, D. T. Moore, J. C. Nino, P. S. Halasyamani, K. R. Poeppelmeier. *J. Am. Chem. Soc*., 2012, **134**, 7679.
12 G. H. Zou, Z. J. Ma, K. C. Wu, N. Ye, *J. Mater. Chem*., 2012, **22**, 19911.
13 T. M. Figueira-Duarte, J. Clifford, V. Amendola, A. Gegout, J. Olivier, F. Cardinali, M. Meneghetti, N. Armaroli, J.-F. Nierengarten, *Chem. Commun*., 2006, **19**, 2054.
14 M. Chen, K. P. Ghiggino, S. H. Thang, G. J. Wilson, *Angew. Chem., Int. Ed*., 2005, **44**, 4368.
15 H. Kang, G. Evmenenko, P. Dutta, K. Clays, K. Song, T. J. Marks, *J. Am. Chem. Soc*., 2006, **128**, 6194.
16 C-Z. Zhang, C. Lu, J. Zhu, C-Y. Wang, G-Y. Lu, C-S. Wang, De-L. Wu, F. Liu, Y. Cui, *Chem. Mater*., 2008, **20**, 4628.
17 C. B. Aakeröy, K. R. Seddon, *Chem. Soc. Rev*., 1993, **22**, 397.
18 D. Xue, S. Zhang, *J. Phys. Chem. Solids*, 1996, **57**, 1321.
19 D. Xue, S. Zhang, *J. Phys. Chem. A*, 1997, **101**, 5547.
20 S. R. Marder, J.W. Perry, C. P. Yakymyshy, *Chem. Mater*., 1994, **6**, 1137.
21 Y. zhou, S. Aravazhi, A. Schneider, P. Seiler, M. Jazbinsek, P, Günter, *Adv. Funct. Mater.*, 2005, **15**, 1072.
22 P.-J. Kim, J.-H. Jeong, M. Jazbinsek, S.-B. Choi, I.-H. Baek, J.-T. Kim, F. Rotermund, H. Yun, Y. S. Lee, P.r Günter, O-P. Kwon, *Adv. Funct. Mater*., 2012, **22**, 200.
23 G. A. Babu, R. P. Ramasamy, P. Ramasamy, V. K. Kumar, *Cryst. Growth Des*.,2009, **9**, 3333.
24 R. Masse, J. Zyss, *Mol. Eng*., 1991, **1**, 141.
25 J. Pecaut, Y. Lefur, R. Masse, *Acta Crystallogr., Sect. B: Struct. Sci*. 1993, **49**, 535.
26 J. Zyss, R. Masse, M. Bagieu-Beucher, J. P. Levy, *Adv. Mater*., 1993, **5**, 120.
27 J. Zaccaro, F. Lorutb. A. Ibaneza, *J. Mater. Chem*., 1999, **9**, 1091.
28 H. Koshima, M. Hamada, Ichizo Yagi, K, Uosak, *Cryst. Growth Des*., 2001, **1**, 467.
29 Y. Fur, M. Bagieu-Beucher, R. Masse, J.-F. Nicoud, J.-P. Lévy, *Chem. Mater*., 1996, **8**, 68.
30 J. Pecaut, J. P. Levy, R. Masse, *J. Mater. Chem*., 1993, **3**, 999.
31 S. Manivannan, S. Dhanuskodi, K. Kirschbaum, S. K. Tiwari, *Cryst. Growth Des*., 2005, **5**, 1463.
32 J. Pecaut, R. Masse, *J. Mater. Chem*., 1994, **4**, 1851.
33 Y. Le Fur, R. Masse, J.-F. Nicoud, *New J.Chem*., 1998, **22**, 159.
34 J.-F. Nicoud, R. Masse, C. Bourgognea, Cara. Evansa, *J. Mater. Chem*., 1997, 7, 35.
35 H. Koshima, H. Miyamoto, I. Yagi, K. Uosaki, *Cryst. Growth Des*., 2004, **4**, 807.
36 G. M. Sheldrick, SHELXL-97 , University of Gottingen, Germany, 1997.
37 M. S. Pandian, P. Ramasamy, *J. Cryst. Growth*, 2010, **312**, 413.
38 S. K. Kurtz and T. T. Perry, *J. Appl. Phys*., 1968, **39**, 3798.
39 O-P. Kwon, S.-J i Kwon, M. Jazbinsek, F. D. J. Brunne r, J.-In Seo, C. Hunziker, A. Schneider, H. Yun, Y.- S. Lee, P. Günter, *Adv. Funct. Mater*., 2008, **18**, 3242.

Journal of Materials Chemistry C Accepted Manuscript

 This journal is © The Royal Society of Chemistry 2012

40 J. Zyss, in *Nonlinear Optics* (Ed.: S. Miyata), Elsevier, Amsterdam, 1992, pp. 33; The definition of $\left\|\beta_{abc}(-2\omega,\omega,\omega)\right\|^2 = \beta_{xxx}^2 + \beta_{yyy}^2 + \beta_{zzz}^2 + 3(\beta_{xyy}^2 + \beta_{yxx}^2 + \beta_{xzz}^2 + \beta_{zxx}^2 + \beta_{yzz}^2 + \beta_{zyy}^2) + 6\beta_{xyz}^2$.

41 W.-D. Cheng, D.-S. Wu, H. Zhang , X.-D. Li, D.-G. Chen, Y.-Z. Lang, Y.-C. Zhang, Y.-J. Gong, *J. Phys. Chem. B*, 2004, **108**, 12658.

42 R. W. Boy, *Nonlinear Optics*; Academic Press: San Diego, CA, 1992, p148.

43 W. Wu, D. Wu, W-D. Cheng, H. Zhang, J. Dai, *Cryst. Grwoth Des.*, 2007, **7**, 2316.

Table of contents (TOC)

Strong Enhancement of Second Harmonic Generation in the Nonlinear Optical Crystals: 2-Amino-3-nitropyridinium Halides (Cl, Br, I)

Tianliang Chen, Zhihua Sun, Xitao Liu, Jinyun Wang, Yuelan Zhou, Chengmin Ji, Shuquan Zhang, Lina Li, Junhua Luo,* Zhong-Ning Chen

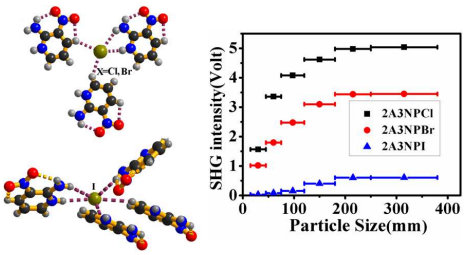

A strong enhancement of nonlinear optical activities in 2-amino-3-nitropyridinium halides have been achieved by choosing moderate anions.

Journal of Materials Chemistry C Accepted Manuscript